



# Numerical studies on fire development inside the corridor

Deepak Sahu<sup>1</sup> · Anchal Bahman<sup>1</sup> · Bhisam Kumar Dhurandher<sup>2</sup> · Amit Rai<sup>3</sup> · Ravikant R. Gupta<sup>4</sup>

Received: 6 July 2021 / Revised: 12 March 2022 / Accepted: 4 June 2022

© The Author(s) under exclusive licence to The Society for Reliability Engineering, Quality and Operations Management (SREQOM), India and The Division of Operation and Maintenance, Lulea University of Technology, Sweden 2022

**Abstract** Fire hazard is one of the major causes of fatalities in the industries and residential areas. The fire hazard in corridors/chambers is caused by the rapid rise of temperatures and presence of high concentrations of toxic gases like CO and smoke. In this study, numerical simulation is conducted with different ventilation conditions to investigate fire behaviour inside the confined area. Fire Dynamic Simulator (FDS) is used for fire simulation studies to predict the fire behaviour inside the corridor. Further, the pyrolysis model is incorporated to study the rate of evaporation of heptane liquid fuel on burning. The size of corridor is 2.5 m long, 1.5 m wide and 1 m high. The vent is at front and back wall to provide the cross-ventilation conditions in case of Test 1. In Test 2 condition, both vents is closed only 5 cm gap has been provided at the centerline of back wall and test 3 one side closed (back wall). The test room is constructed with concrete and bricks. The fire source is created at the corner of the corridor using heptane fuel. The heat release rate, temperature at the different locations: at ceilings and vents and velocity and concentration of O<sub>2</sub>, CO<sub>2</sub>, and CO are predicated at different test conditions. The maximum heat release rate is found to be 62 kW, 45 kW, and 69 kW in Test 1, Test 2, and Test 3 respectively. The maximum temperature is found to be 92 °C, 215 °C and 152 °C near to fire source

in case of Test 1, Test 2 and Test 3 respectively. In Test 2, has low ventilation conditions, oxygen gets limited to 6%, however in case of Test 1 and Test 3 it maintains at 18% during the test period.

**Keywords** FDS · Combustion modeling · Liquid fuel · Enclosure

## 1 Introduction

The need for homes and commercial structures is increasing as the world's population grows and globalization takes hold. Buildings, on the other hand, lack adequate fire suppression systems to avoid fire hazards if any accident occurs. Rapid temperature rises, as well as high concentrations of poisonous gases such as CO and smoke, contribute to a fire hazard in a building. Smoke can greatly limit visibility, making it more difficult for individuals to see.

Fires are major disaster causing high fatalities even on the slightest spark. The occurrence of fire requires three primary prerequisites: substance (combustible material, i.e., solid, liquid, and gas), oxidant (oxygen, hydrogen peroxide (H<sub>2</sub>O<sub>2</sub>), fluorine (F<sub>2</sub>), nitric acid, etc.), and suitable environment (ignition source, temperature).

Delichatsios et al. (2009) estimated measuring enclosure gas temperature in an under-ventilated enclosure with the dimensions of 0.8 m × 1.2 m × 0.8 m using Industrial Methylated Spirit (IMS). Newman and Xin (2004) used heptane and propylene as fuel to analyze the fire behavior in an enclosure with dimensions of 18.29 m × 12.19 m × 6.10 m. The combustion product distribution and temperature were derived and validated by them using scale modeling for larger enclosures. Meroney et al. (2015) suggested a new ventilation system for removing flammable gases from a room.

✉ Deepak Sahu  
sahud@nitj.ac.in

<sup>1</sup> Chemical Engineering Department, Dr. B R Ambedkar National Institute of Technology Jalandhar, Jalandhar, India

<sup>2</sup> School of Mechanical Engineering, VIT Chennai, Chennai, India

<sup>3</sup> Department of Chemical Engineering, SLIET, Longowal, District, Sangrur, Punjab, India

<sup>4</sup> Department of Chemical Engineering, Banasthali University, Banasthali Vidyapith, District, Tonk, Rajasthan, India

Oka and Oka (2017) used an LES research with the Smagorinsky Model and the model constant-coefficient at Sub Grid-Scale (SGS) to quantitatively analyze the plume properties. By changing the fuel source position, the excess temperature and the influence of amplitude of oscillation on the fire plume created were determined. Beji et al. (2018) investigated the LES model for hot air and water spray encounters (two-phase flow). The sensitivity of the computational domain and mesh for three cell sizes of 2 mm, 4 mm, and 8 mm was evaluated. In the Smagorinsky model, three stages were tackled: impinging a vertical jet on a horizontal plate, characterizing water strays, and sprat jet contact.

Chen et al. (2016) evaluated the fire behavior inside an enclosed area with a ceiling vent using numerical modeling. The effect of the size of the opening on heat release rate was studied using a 3 m × 2 m × 2 m box and heptane as the fuel. The size of the opening of the ceiling vent was increased; the rate of heat emission also rises. Dhurandher et al. (2017) carried out an experimental investigation using plywood cribs as fuel found that a sharp rise in ventilation caused a 150% increase in fuels mass loss rate, resulting in a 198 kW increase in the heat loss rate.

Hwang et al. (2010) investigated the temperature and flow characteristics within an ISO9705 room in both over and under-ventilated circumstances using heptane as a fuel. In case of over ventilated fire settings, uniform distribution of temperature and combustion products was detected under low HRR settings, whereas a change in the profile of flame was seen under high HRR situations.

Hu et al. (2007) undertook a full-scale experiment in an underground channel of 88 m × 8 m × 2.65 m. He used a diesel pool with a maximum stable HRR of 0.75 MW and 1.6 MW as fire a source in the tests. The concentration of CO was increased linearly with height above the floor and falls exponentially with channel length.

Hu et al. (2008) studied the back-layering position and critical velocity in turner fires. The back layer length was depended on ventilation condition, height of tunnel and pool size. The back layer length increases with pool size and decreased with longitudinal velocity.

Zhang et al (2014) studied the smoke exhaust system in a corridor, which is extremely important for electrical power transmissions. The smoke extraction system was affected with height and airflow inlet positions.

CFD simulation was done by Zhang et al. (2015) on a corridor model. In the first case, the fire was placed in the lower corridor and in another case; the fire was placed at the upper level. The second case was found to be more dangerous, because of buoyancy and airflow through the doors, smoke descends and creates a more hazardous situation. The critical velocity of airflow was required to control the spread of smoke using Froude modeling.

Zhou et al. (2017) performed corridor and scale model to carry out simulations on a larger scale (4:1) found that the larger trays led to more HRR, which subsequently to more vertical temperature. However, the temperature declines along the length of the corridor.

Wua et al. (2018) conducted reduce scale numerical simulations (1:4) for a tunnel fire without train blockage. Experiments were conducted to measure the smoke layer length under different conditions. Variations in three parameters are studied- HRR, longitudinal ventilation velocities, and ambient pressure conditions. The smoke layer was decreases with an increase in ambient pressure conditions, keeping the ventilation velocity and HRR constant.

The numerical simulation studies (Cai and Chow 2014) on room fires were conducted for different grid sizes and boundary conditions to analyze the effect on predicted results. Wang et al. (2018) studied the control of smoke and CO transportation in channel fire using Water Mist Curtain (WMC) system. They were found that WMC system effectively decrease the temperature even under low working pressure.

Sahu et al. (2019) were performed experimental studies on different liquid fuel fire inside the enclosure. The burning behavior of fuel was significantly depended on properties of fuel such as heat of combustion, vaporization rate and sootiness. Smoke production rate and concentration of CO and CO<sub>2</sub> were depended on nature of fuels.

Chotzoglou et al. (2019) investigated the liquid pool fire inside the corridor of size 3 m × 0.5 m × 0.5 m. The burning behavior of liquid under different regions fuel-controlled, ventilation-controlled and steady-state burning were studied. The difference of burning rate in corridor and cubic shape enclosure was clearly observed by Chotzoglou et al. The HRR inside the corridor in case of the ventilation-controlled fires was found lower than the value  $1500AoHo^{1/2}$  used for rectangular compartments.

The burning behaviors of liquid fuel fire were mostly studied on cubical shape of enclosure, where, thermal distribution was normally uniform. However, less information available on burning rate, thermal and toxic gases distribution in corridor like enclosure. Corridors are common in industries and residential areas. The lack of knowledge and drastic changes in structures and process causes of fire. This motivates to invent methods and techniques to understand the behavior of fire.

The idea of this research is to explore the fire behaviour in a corridor. The present simulation studies are performed on reduced scale corridor like enclosure to investigate the fire behavior, where corridor length 2.5 m, width of 1.5 m, and a height of 1 m, also studies the impact of ventilation under cross ventilation conditions. The most of previous research were performed with gaseous burners, where, fuel supply rate was pre-defined.

The present studies are focused on more common hydrocarbon fuel heptane, which is widely used in the automobile industry. Also, use as a fuel due to its high flammability, thinner for cement industry and solvent for laboratory purposes. Furthermore, the properties of heptane fuel such as boiling temperature, vapor pressure, heat of combustion are constant as compare to others multi-constituent fuels. Moreover, fuel supply rate is not controlled by pre defined supply rate. The FDS code is used to quantify the HRR and Mass burning rate, temperature and concentration of product gases.

## 2 Methodology

### 2.1 Geometry and domain creation

Preprocessing of CFD modeling includes defining the region of problem, creation of computational domain, grid and meshing. Further, it includes defining physics of problem i.e. physical and chemical phenomena, details of the properties of fluid and obstructions, and selecting appropriate boundary condition.

The first step of the model is to create the geometry of the problem. The computational domain is extended from boundary of test room to overcome the disturbance problem at the inlet of the test room. The computational domain of the model is based on characteristic fire diameter as had been described by McGrattan et al., 2010 and He et al., 2018. The size of mesh cell  $\delta x$  is calculated form characteristic fire diameter  $D^*$  as defined in Eq. 1

$$D^* = \left( \frac{\dot{Q}}{\rho_\infty C_p T_\infty \sqrt{g}} \right)^{2/5} \tag{1}$$

Here,  $\dot{Q}$  is heat release rate (kW);  $\rho_\infty$  is ambient air density ( $\text{kg/m}^3$ );  $C_p$  specific heat of air (kJ/kg K);  $T_\infty$  is ambient temperature (K);  $g$  is gravitational acceleration ( $\text{m/s}^2$ ).

The grid sensitivity study is performed on Test 1 condition, which helps to investigate the effect of meshing on predicted results. In the present work characteristic fire diameter is found 0.29 based on maximum heat release rate. The mesh sizes are selected based on the ratio of  $D^*/\delta x$ . The ratio of  $D^*/\delta x$  is found 3, 5 and 8 in the case of sim.1, sim.2, sim.3 and sim.4 conditions respectively.

### 2.2 Selection of physical sub-models

Numerical simulations have been performed using CFD tool—Fire Dynamic Simulator (FDS) version 6.0.1, developed by NIST, USA. Hydrodynamic Model, Combustion Model and Radiation Transport model are used in FDS for

simulating the fire dynamics. In Hydrodynamic model, turbulence is treated by means of the Smagorinsky form of Large Eddy Simulation (LES). LES model is used to understand the local turbulence due to mixing of the gaseous fuel and product gases in the local environmental condition.

Combustion model is based on mixture fraction (of fuel and air) concept to predict the extent of combustion. In Radiation Transport model, the solution of the radiation transport equation for a gray gas is solved using finite volume method.

McGrattan et al. (2015) suggested a pyrolysis model; study the rate of evaporation of liquid fuels on burning. The model is worked on Clausius-Clapeyron relation as defined in Eq. 2 to predict the volume fraction of the fuel vapor ( $X_F$ ), depends on boiling temperature ( $T_b$ ) and heat of vaporization of liquid ( $h_v$ ). The temperatures and velocities distributions inside the enclosure are predicted under different ventilation and boundary conditions.

$$X_F = \exp \left[ \left( \frac{-h_v W}{R} \right) \left( \frac{1}{T_s} - \frac{1}{T_b} \right) \right] \tag{2}$$

where vaporization heat  $h_v$ , molecular weight  $W$ , surface temperature  $T_s$ , and boiling temperature  $T_b$ , gas constant  $R$ .

## 3 Numerical configurations

Figure 1 shows the small scale Test model of the corridor with dimensions  $2.5 \text{ m} \times 1.5 \text{ m} \times 1 \text{ m}$ ; both sides are open, enabling a cross-ventilation situation. The corridor walls are made of cemented bricks and thickness of 0.1 m. The ceiling and floor are made of concrete and thickness of 0.1 m.

Heptane fuel is taken as a fire source and it is kept at the corner of the corridor at a location of  $x=0.1 \text{ m}$ ,  $y=0.1 \text{ m}$ . The pool area is  $0.17 \text{ m} \times 0.17 \text{ m}$  with depth of 12 cm. The fire source is created inside the chamber/corridor allow to burn initially. The details of the Test model and simulation conditions are summarized in Tables 1 and 2.

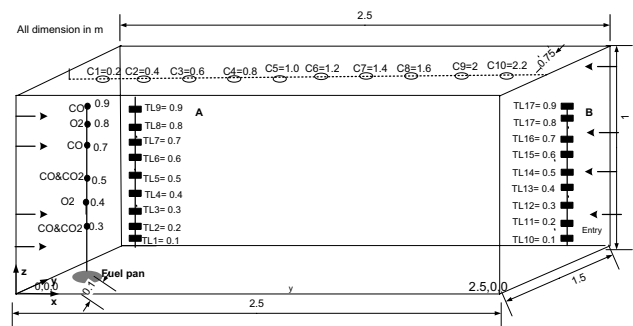


Fig. 1 Test Layout

**Table 1** Summary of Test model conditions

Test No	1	2	3
Size of vent: width (m)×height (m)	1×1.5 (Cross Ventilation)	5 cm gap (x=2.5, y=0.7–0.75, z=1)	1.5 m×1 m
Ventilation condition	Both vent open	Vent closed, only main- tain 5 cm gap	One end is open at (x=0, y=0, z=0)
Size of Corridor 2.5 m×1.5 m×1 m			

**Table 2** Details of simulation parameter

Parameters	Test1	Test 2	Test 3
Initial temperature (°C)	20	20	20
Simulation type	LES, Transient		
Computational domain	3.5 m×1.8 m×1.3 m		
Total simulation time (s)	500		
Cell size (m)	0.04×0.04×0.04		
Total cell	150,000		
Turbulence	Smagorinsky model		
Smagorinsky constant	0.2		
Radiation loss fraction	0.25		
Fire source	Pyrolysis of heptane		
Grid sensitivity analysis for Test 1			
Test 1	Cell size	Total cell	
Sim. 1	0.10 m×0.09 m×0.06 m	14,000	
Sim. 2	0.06 m×0.06 m×0.06 m	36,000	
Sim. 3	0.04 m×0.04 m×0.03 m	128,000	
Sim. 4	0.04 m×0.04 m×0.04 m	150,000	

*Sim.*, Simulation

Temperature and concentration of O<sub>2</sub>, CO and CO<sub>2</sub> are measured continuously throughout the corridor. Details of sensors located at different locations inside the corridor are summarized in the Table 3.

The thermocouple's rack (A) and (B) are fixed in the corner of corridor to predict the temperature distribution along the height of corridor. The thermocouples rack "A" (TL1—TL9) is fixed at the corner (x=0.2 m, y=1.3 m) with the increment of 0.1 m height and another thermocouples rack "B" (TL10—TL17) is fixed at the corner (x=2.4 m, y=1.3 m) with the increment of 0.1 m height of the corridor to predict the temperature distribution along with the heights of the corridor.

Another set of thermocouples C1 to C10 fixed at center-line of corridor at y=0.75 to measure the temperature of hot gases along the length of ceiling with increment of 0.2 m.

Two oxygen sensors are placed above the fuel surface to predict the oxygen concentration availability for the

fuel-burning at a location of x=0.13 m, y=0.13 m, z=0.4 and z=0.8. Similarly, CO sensors are fixed at the location of (x=0.13 m, y=0.13 m, with height of z=0.3 m, 0.5 m, 0.7 m and 0.9 m) to measure the concentration of CO gases during a fire. The sensor CO<sub>2</sub> are fixed at a locations of (x=0.13 m, y=0.13 m, with height of z=0.3 m, and 0.5 m) to predict the CO<sub>2</sub> gas.

A corner fire experimental study is conducted on Test 1 conditions. Here, simulation studies of Test 1 under different grid have compared with experimental value for validation of simulation parameters.

Grid sensitivity studies have been done in the case of Test 1, the predicted value of heat release rate under different grid as shown in Fig. 2. In simulation 4, the heat release rate is found to be closed with the experimental value, where size of the grid is 0.4 m×0.4 m×0.4 m and the Total cell is 150,000. Therefore, grid size of simulation 4 condition has considered as most effective for further study.

**Table 3** Details of sensors located at different location inside the corridor

x	y	z	Sensors
<i>CO sensors</i>			
0.13	0.13	0.3	CO
0.13	0.13	0.5	CO
0.13	0.13	0.7	CO
0.13	0.13	0.9	CO
<i>CO<sub>2</sub> sensors</i>			
0.13	0.13	0.3	CO <sub>2</sub>
0.13	0.13	0.5	CO <sub>2</sub>
<i>O<sub>2</sub> sensors</i>			
0.13	0.13	0.4	O <sub>2</sub>
0.13	0.13	0.8	O <sub>2</sub>
<i>Thermocouples position at corner A</i>			
0.2	1.3	0.1	T <sub>L1</sub>
0.2	1.3	0.9	T <sub>L9</sub>
<i>Thermocouples positions at corner B</i>			
2.4	1.3	0.1	T <sub>L10</sub>
2.4	1.3	0.9	T <sub>L18</sub>
<i>Thermocouples positions at ceiling</i>			
0.2	0.75	0.8	TC1
2.2	0.75	0.8	TC10

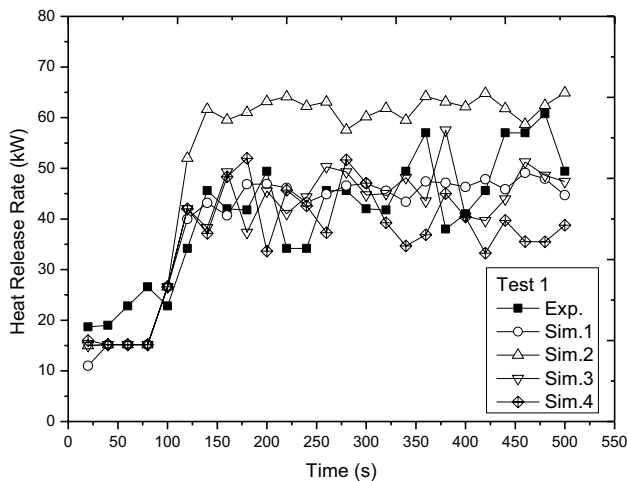


**Fig. 2** Variation of Heat release rate with time under different grid in case of Test 1

### 4 Results and discussion

The variation of heat release rate with time under different vent conditions is shown in Fig. 3. The fire growth continues up to 50 s before it achieved a steady value. The maximum heat release rate (HRR) is found to be 62 kW, 45 kW, and 69 kW in Test 1, Test 2, and Test 3 respectively. The development of fires inside the confined area is depended on the

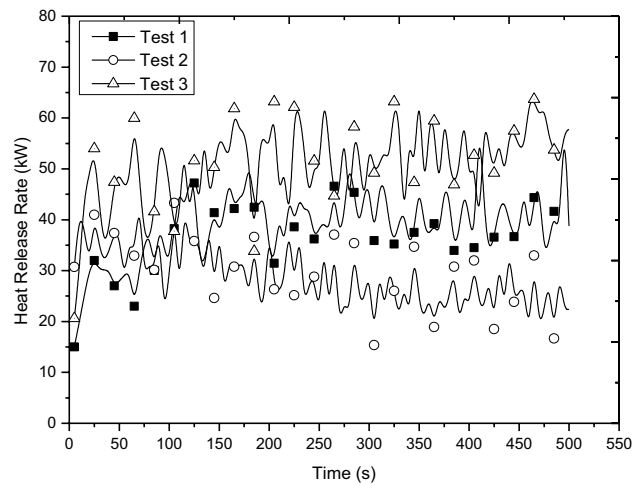


**Fig. 3** Variation of Heat Release Rate with time under different vent conditions

availability of oxygen and also by the heat feedback to the fuel surface.

The fire inside the compartment is mostly affected by the hot gas layer, which is radiated heat towards the fuel surface, as a result enhancing the burning rate. In present test 1- 3, at the beginning of burning of fuel is increased rapidly by heat feedback. The enclosure vents (doors, windows, leakage areas) may restrict the availability of oxygen needed for combustion.

The maximum heat release rate is predicted in Test 3 due to high feedback and lesser cooling effect. However, the lowest value is found in Test 2, due to the low availability of oxygen and it is reduced abruptly in Test 2 due to lack of ventilation.

Oxygen depletion inside the corridor is shown in Fig. 4. The profile of oxygen is predicted at a height of 0.4 m and 0.8 m above the fuel surface. At a height of 0.4 m above the fuel surface, the oxygen concentration in the case of Test 2 is depleted more as compare to Test 1 and Test 3, resulting in the formation of CO and reduction in burning rate or heat release rate. The effects of ventilation are observed in Test 1–3. Another effect of ventilation is seen higher in test 3, where oxygen concentration is sufficient for sustaining the burning of heptane. In Test 1, oxygen is sufficient but excess cooling effects have been observed.

Oxygen depletion inside the corridor at a height of 0.8 m above the fuel surface is shown in Fig. 5. The concentration of Oxygen is predicted same in both Test 1 and Test 3, whereas in Test 2 conditions, it is found a different and the lowest values as compare to Test 1 and Test 2. From, Figs. 4 and 5, it can be understood that the concentration vary with height and time inside the corridor.

Figures 6 and 7 shows the concentration of CO<sub>2</sub> in the upper and lower zone of the corridor under different

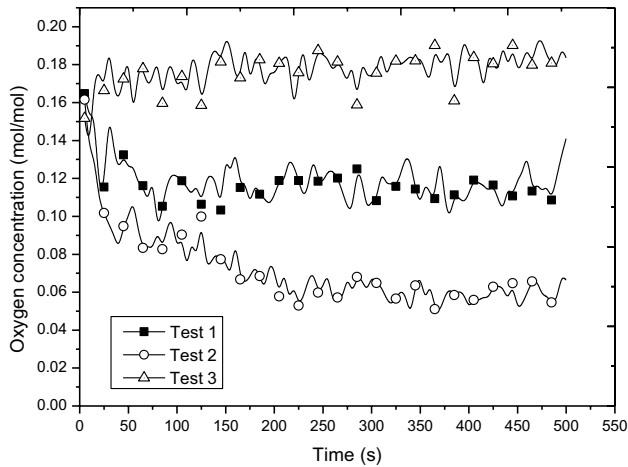


**Fig. 4** Concentration of Oxygen gas inside the corridor at height of 0.4 m above the fuel surface

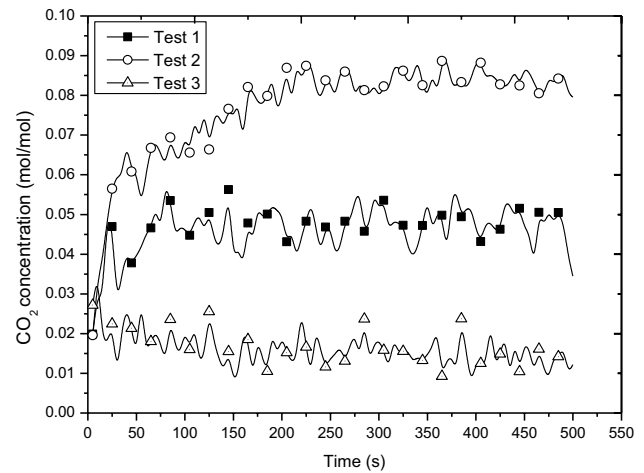


**Fig. 6** Concentration of CO<sub>2</sub> gas inside the corridor at height of 0.3 m above the fuel surface

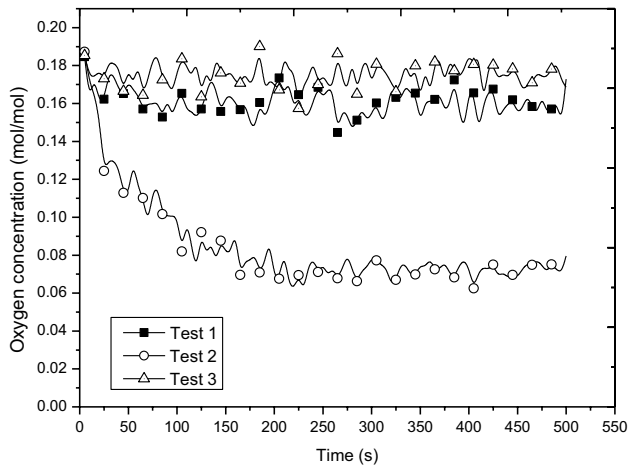


**Fig. 5** Concentration of Oxygen gas inside the corridor at height of 0.8 m above the fuel surface

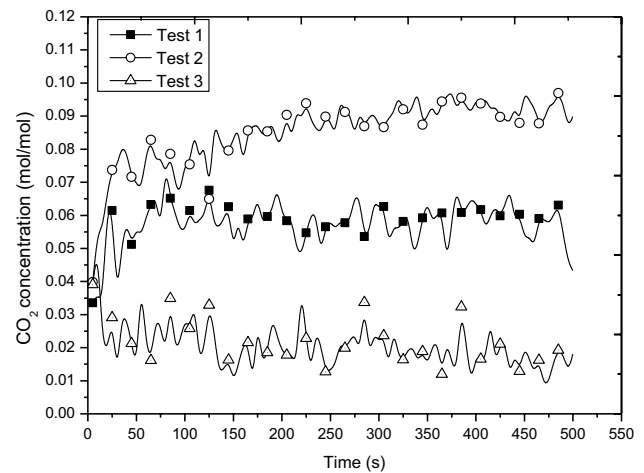


**Fig. 7** Concentration of CO<sub>2</sub> gas inside the corridor at a height of 0.5 m above the fuel surface

ventilation conditions and time. The formation of CO<sub>2</sub> is increasing with time as a burning proceeds and found similar profile with heat release rate. The profile of product gases is found to be similar in both zones of the corridor.

Figure 8 shows the variation of CO concentration inside the corridor with the heights of the corridor under different vent conditions at a time of 300 s. The Concentration of CO has resulted higher in Test 2 as compare to Test 1 and Test 3, due to depletion of oxygen and incomplete combustion. This represents the low burning rate and high production rate of CO. This value has resulted higher at a distance of 0.3 m above the fuel surface, where O<sub>2</sub> depletion is more.

Figure 9 shows the variation of corner temperature at different heights from the floor under different vent locations. Section "A" represents the thermocouple tray at X=0.2 m,

Y = 1.3 m. Similarly, for Section "B" which is located at X = 2.4 m, Y = 1.3 m. The corridor has distinguished into two zones i.e., hot and cold zone in both sections of the corridor. This layer is found at a height of 0.4 m above the floor in Test 1 and Test 3. However, in the case of Test 2, there is no distinction found in the lower and upper zone due to smoke filling inside the corridor, a single zone model is predicted. The maximum temperature at a location of the cold zone is found about 22 °C and 24 °C in Test 1 and 3, and the upper zone temperature is found to be 102 °C and 152 °C. There are differences observed in sections "A" and "B" due to lateral air entrainment and flame radiation effects at the location of Section "A" as compared to "B".

Figure 10 shows the variation of mean ceiling temperature along the length of the corridor under different vent

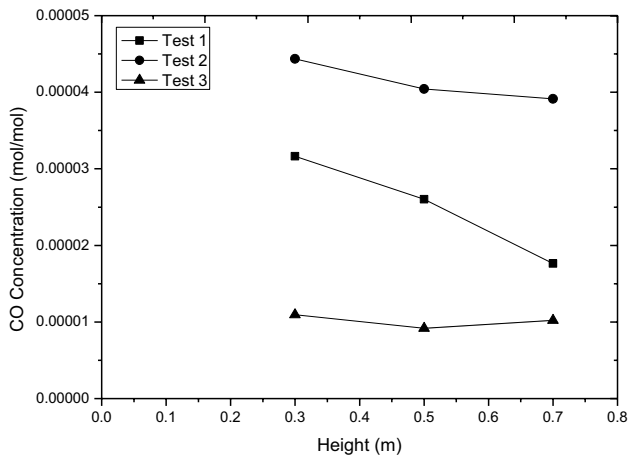


Fig. 8 Variation of CO gas concentration inside the corridor at the different height at time of 300 s

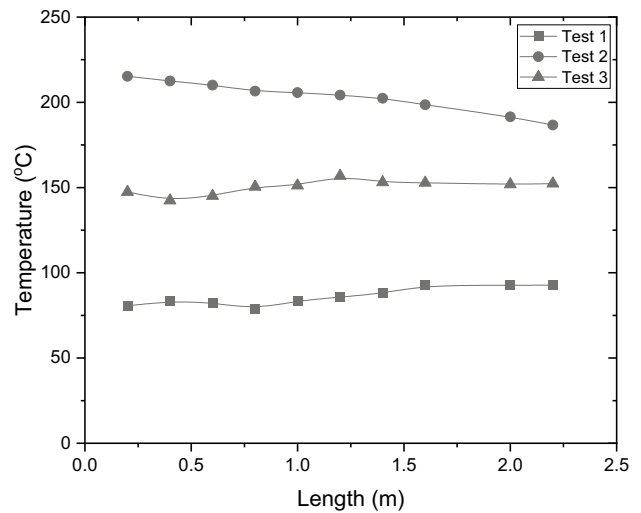


Fig. 10 Variation of Ceiling temperatures at 0.2 m below the ceiling at a different location at the time of 300 s

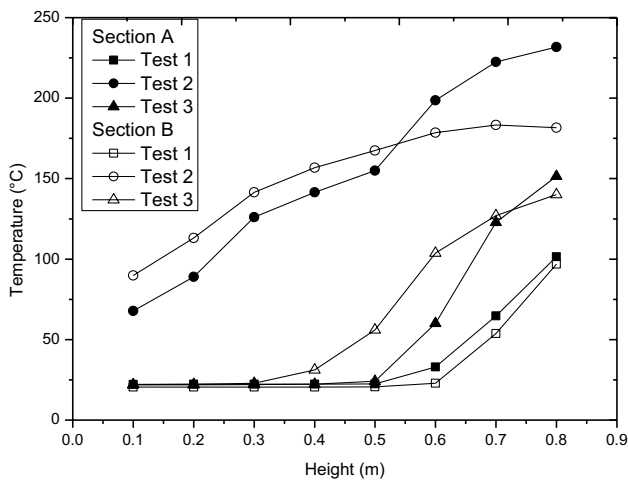


Fig. 9 Variation of temperatures along with the height of corridor under different ventilation conditions at the time of 300 s

conditions at time of 300 s. There is non- uniformity in temperature development found along the length of the corridor. The maximum temperature is found to be 92 °C, 215 °C, and 152 °C near to fire source in the case of Test 1, Test 2, and 3 respectively. Whereas, maximum temperature difference along the length of the corridor is found to be approximately 12 °C, 29 °C, and 5 °C. It is clear from this figure that the hot gas layer is not uniform in Test 1 and Test 2 conditions.

Figure 11 shows the velocity profile at  $x=0, y=1.0$  inside the corridor under different test conditions at a time of 300 s. It is predicted that the velocity field increases with decreases the vent, which may results in high turbulence at low ventilation conditions. It is inferred from a profile that mixing of hot gases with cold air has resulted higher in Test 2 and non-uniform distribution.

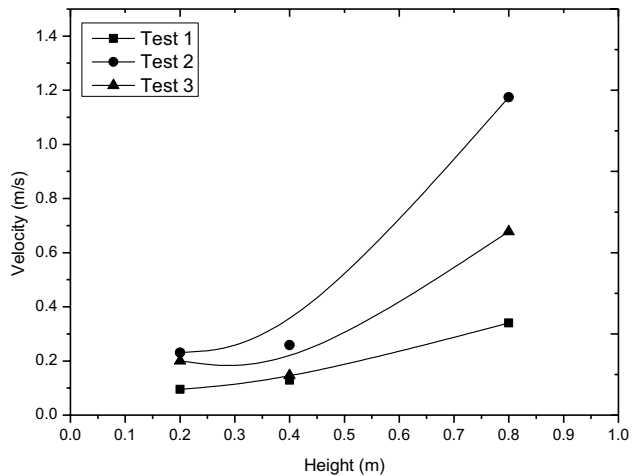
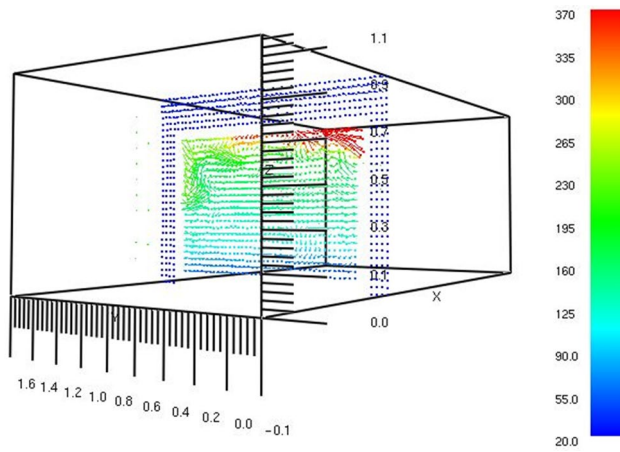
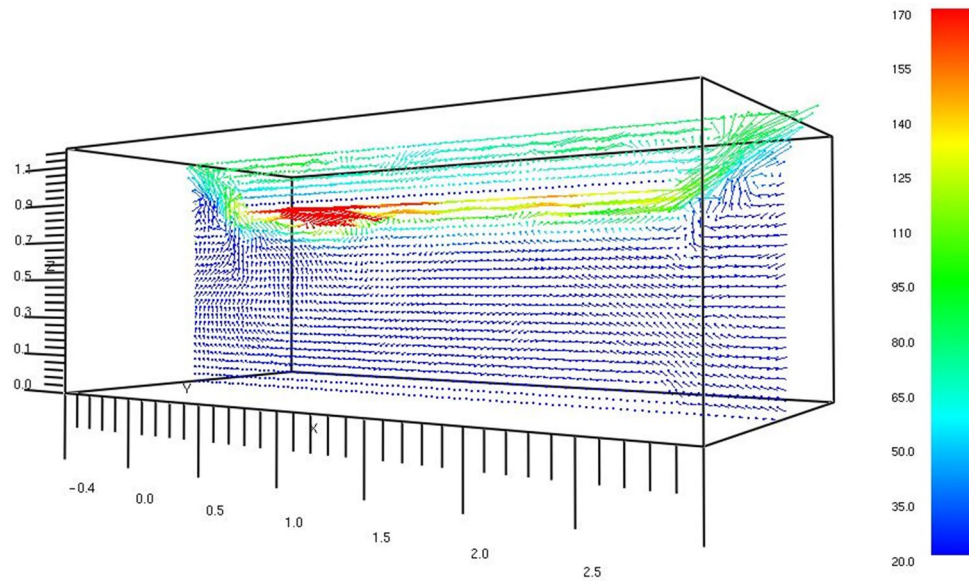


Fig. 11 Velocity profile under different vent conditions at the time of 300 s

Figures 12, 13 and 14 show the temperature field inside the corridor at a time of 300 s in the case of Test1, Test 2 and Test 3 respectively. These results are helped to understand the different ranges of temperature along the lengths and heights of the corridor.

Figures 15, 16 and 17 show the smoke distribution inside the corridor under different Test 1, Test 2 and Test 3 conditions respectively. At the beginning of the fire, the smoke is accumulated at the ceiling and thereafter it's filling to the corridor. In Test 2, the smoke filling rate is observed fast as compared to Test 1 and Test 3. In Test 2, the whole corridor is filled with smoke layer at a time of 100 s after ignition. The smoke layer can significantly reduce visibility thus affected the possibility for the people to reach escape routes.

**Fig. 12** Temperature distribution ( $^{\circ}\text{C}$ ) inside the corridor at the time 300 s in Test 1



**Fig. 13** Temperature distribution ( $^{\circ}\text{C}$ ) inside the corridor at the time of 300 s in Test 2

## 5 Conclusion

The present studies specially focused on to investigate the heat release rate, thermal environment, and concentration of

product gases. The results have shown that burning behavior changing significantly in different vent conditions in a corridor. The oxygen availability gets limited after a time period of 50 s in Test 2 conditions. The production of CO gas resulted higher in the case of Test 2 as compare to Test 1 and Test 3. The development of temperature has resulted higher in low vent test conditions, i.e., Test 2. The maximum ceiling temperature differences between Test 2 and Test 1 are found  $122^{\circ}\text{C}$  and similarly for Test 2 and Test 3 is  $58^{\circ}\text{C}$ . Safety of person is a critical factor whenever a fire accident takes place in underground station or corridor types areas because of limitation of ventilation systems to provide a safer indoor environment and extraction of the smoke and hazardous gasses. The results will be useful in the understanding the thermal, smoke and toxic gases distribution in the corridor type enclosure. The propagation of smoke in the corridor is fast due to their narrow and long shape, which can show the way to catastrophic results. The smoke can significantly reduce the visibility thus reducing the possibility for the people to reach escape routes.



**Fig. 14** Temperature distribution (°C) inside the corridor at time 300 s in Test 3

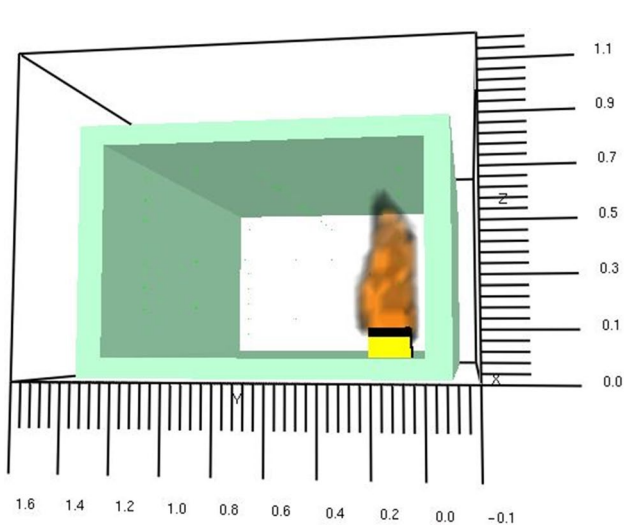
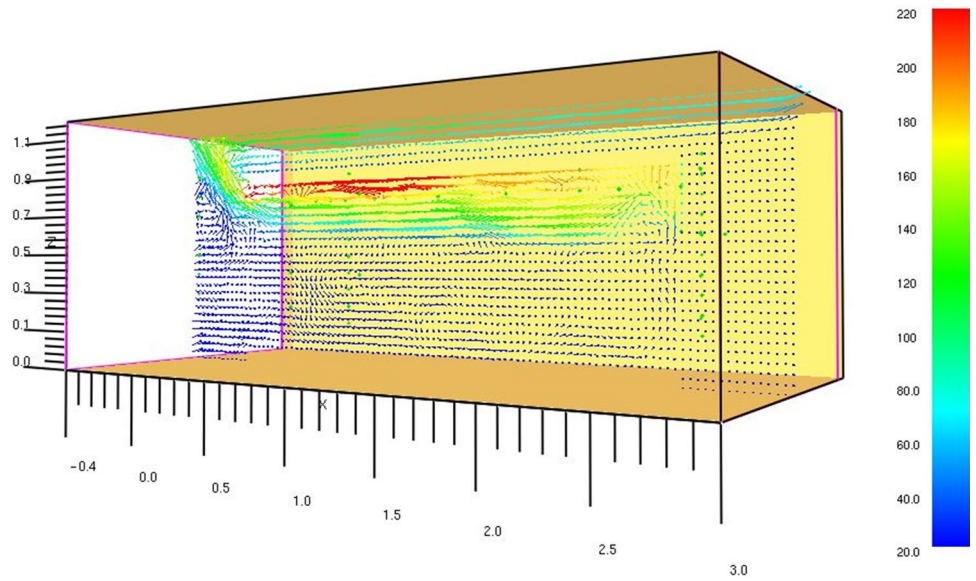


**Fig. 15** Smoke distribution in Test 1 at the time of 300 s

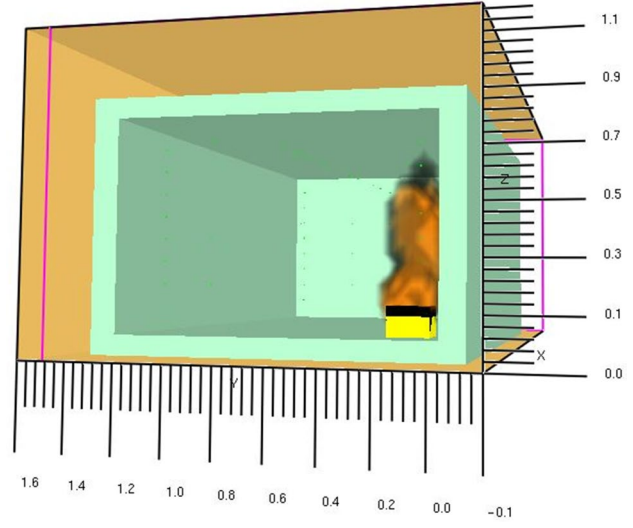


**Fig. 17** Smoke distribution in Test 3 at the time of 300 s

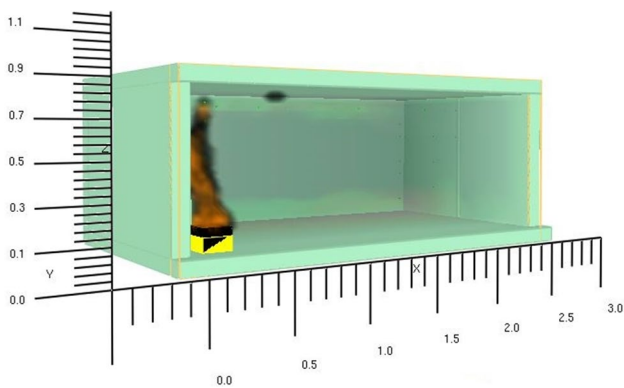


**Fig. 16** Smoke distribution in Test 2 at the time of 300 s

**Acknowledgements** The authors acknowledge the Late Prof. Shashi for her guidance, Department of Chemical Engineering, IIT Roorkee, Roorkee, India.

**Funding** There is no funding provided for the preparation of manuscript.

**Declarations**

**Conflict of interest** The authors declare that there is no conflict of interests.

## References

- Beji T, Maragos G, Ebrahimzadeh S, Merci B (2018) Numerical modelling of the interaction between water sprays and hot air jets—part I: gas phase large eddy simulations. *Fire Saf J* 95:77–86. <https://doi.org/10.1016/j.firesaf.2017.11.005>
- Cai N, Chow W (2014) Numerical studies on heat release rate in a room fire burning wood and liquid fuel. *Build Simul* 7:511–524. <https://doi.org/10.1007/s12273-014-0177-4>
- Chen AQ, Li Q, Wang YG (2016) Investigation of the burning mechanism in an enclosure fire with a horizontal ceiling vent. *Proc Eng* 135:1–11. <https://doi.org/10.1016/j.proeng.2016.01.071>
- Chotzoglou KE, Asimakopoulou EK, Zhang J, Delichatsios M, A, (2019) An experimental investigation of burning behaviour of liquid pool fire in corridor-like enclosures. *Fire Saf J* 108:102826
- Delichatsios MA, Lee YP, Tofilo P (2009) A new correlation for gas temperature inside a burning enclosure. *Fire Saf J* 44:1003–1009. <https://doi.org/10.1016/j.firesaf.2009.06.009>
- Dhurandher BK, Kumar R, Dhiman AK (2017) An experimental study on crib fires in a closed compartment. *Therm Sci* 21(3):1431–1441. <https://doi.org/10.2298/TSCI141206156D>
- He QZ, Yang JT, Zhang YF (2018) Numerical simulation of fire induced gas flow in a narrow ceiling vented compartment. *Proc Eng* 211:226–234. <https://doi.org/10.1016/j.proeng.2017.12.008>
- Hu LH, Fong NK, Yang LZ, Chow WK, Li YZ, Huo R (2007) Modeling fire-induced smoke spread and carbon monoxide transportation in a long channel: Fire Dynamics Simulator comparisons with measured data. *J Hazard Mater* 140:293–298. <https://doi.org/10.1016/j.jhazmat.2006.08.075>
- Hu LH, Huo R, Chow WK (2008) Studies on buoyancy-driven back-layering flow in tunnel fires. *Exp Thermal Fluid Sci* 32:1468–1483
- Hwang CH, Lock A, Bundy M, Johnsson E, Ko GH (2010) Compartments studies on fire characteristics in over and under ventilated full-scale compartments. *J Fire Sci* 28(5):458–485. <https://doi.org/10.1177/0734904110363106>
- McGrattan K, McDermott R, Hostikka S, Floyd J (2010) Fire dynamics simulator (version 5), user's guide, 1019–5. National Institute of Standards and Technology, Gaithersburg, MD, USA
- McGrattan K, Hostikka S, McDermott R, Floyd J, Weinschenk C, Overholt K (2015) Fire dynamics simulator (version 6), technical reference guide. Gaithersburg, MD, USA: National Institute of Standards and Technology
- Meroney RN, Hill DW, Derickson R, Stroup J, Weber K, Garrett P (2015) CFD Simulation of ventilation and smoke movement in a large military firing range. *J Wind Eng Ind Aerodyn* 136:12–22. <https://doi.org/10.1016/j.jweia.2014.10.011>
- Newman JS, Xin Y (2004) Characterization of room environments in growing enclosure fires. *Fire Saf J* 39:239–253. <https://doi.org/10.1016/j.firesaf.2003.11.008>
- Oka H, Oka Y (2017) Numerical analysis on plume temperature properties formed above a harmonically oscillating fire source. *Fire Saf J* 88:56–66. <https://doi.org/10.1016/j.firesaf.2016.12.001>
- Sahu D, Jain S, Gupta A, Kumar S (2019) Experimental studies on different liquid pool fires inside the enclosure. *Fire Safety J* 109:102858–102868
- Wang Z, Wang X, Huang Y, Tao C, Zhang H (2018) Experimental study on fire smoke control using water mist curtain in channel. *J Hazard Mater* 342:231–241. <https://doi.org/10.1016/j.jhazmat.2017.08.026>
- Wua F, Zhou R, Shen G, Jiang J, Li K (2018) Effects of ambient pressure on smoke back-layering in subway tunnel fires. *Tunn Undergr Space Technol* 79:134–142. <https://doi.org/10.1016/j.tust.2018.05.011>
- Zhang Y, Li A, Hu J, Gao R (2014) Prediction of carbon monoxide concentration and optimization of the smoke exhaust system in a busbar corridor. *Build Simul* 7:639–648. <https://doi.org/10.1007/s12273-014-0173-8>
- Zhang B, Zhang J, Lu S, Li C (2015) Buoyancy-driven flow through a ceiling aperture in a corridor: a study on smoke propagation and prevention. *Build Simulation* 8:701–709. <https://doi.org/10.1007/s12273-015-0248-1>
- Zhou J, Mao J, Huang Y, Xing Z (2017) Studies on smoke temperature distribution in a building corridor based on reduced-scale experiments. *J Asian Arch Build Engineering* 16(2):341–348. <https://doi.org/10.3130/jaabe.16.341>

**Publisher's Note** Springer Nature remains neutral with regard to jurisdictional claims in published maps and institutional affiliations.